

AD-A181 130

SMALL SIGNAL ANALYSIS OF THE INDUCED RESONANCE ELECTRON
CYCLOTRON MASER (U) SCIENCE APPLICATIONS INTERNATIONAL
CORP MCLEAN VA S RIVOPoulos ET AL 20 MAY 87
NRL-MR-5986 DE-A185-83ER40117

1/1

UNCLASSIFIED

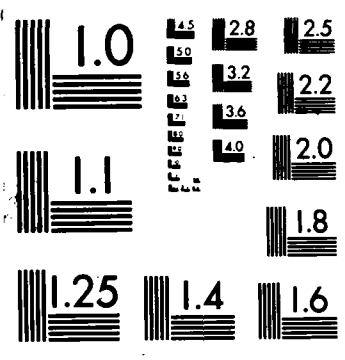
F/G 9/1

NL

FND

187

DIC



DTIC FILE COPY

Naval Research Laboratory

Washington, DC 20375-5000



3

NRL Memorandum Report 5986

AD-A181 130

Small Signal Analysis of the Induced Resonance Electron Cyclotron Maser

S. RIZOPOULOS,* C. M. TANG AND P. SPRANGLE

*Plasma Theory Branch
Plasma Physics Division*

**Science Applications, Intl. Corp., McLean, VA*

May 20, 1987

DTIC
ELECTE
JUN 15 1987
S D

Approved for public release; distribution unlimited.

SECURITY CLASSIFICATION OF THIS PAGE

A181130

REPORT DOCUMENTATION PAGE				
1a. REPORT SECURITY CLASSIFICATION UNCLASSIFIED		1b. RESTRICTIVE MARKINGS		
2a. SECURITY CLASSIFICATION AUTHORITY		3. DISTRIBUTION/AVAILABILITY OF REPORT Approved for public release; distribution unlimited.		
2b. DECLASSIFICATION/DOWNGRADING SCHEDULE		5. MONITORING ORGANIZATION REPORT NUMBER(S)		
4. PERFORMING ORGANIZATION REPORT NUMBER(S) NRL Memorandum Report 5986		7a. NAME OF MONITORING ORGANIZATION		
6a. NAME OF PERFORMING ORGANIZATION Naval Research Laboratory	6b. OFFICE SYMBOL (If applicable) Code 4790	7b. ADDRESS (City, State, and ZIP Code)		
6c. ADDRESS (City, State, and ZIP Code) Washington, DC 20375-5000		9. PROCUREMENT INSTRUMENT IDENTIFICATION NUMBER		
8a. NAME OF FUNDING/SPONSORING ORGANIZATION U.S. Department of Energy	8b. OFFICE SYMBOL (If applicable)	10. SOURCE OF FUNDING NUMBERS		
8c. ADDRESS (City, State, and ZIP Code) Washington, DC 20545		PROGRAM ELEMENT NO DOE	PROJECT NO AT05-83 ER40117	TASK NO ORD (326)
WORK UNIT ACCESSION NO DN380-537				
11. TITLE (Include Security Classification) Small Signal Analysis of the Induced Resonance Electron Cyclotron Maser				
12. PERSONAL AUTHOR(S) Riopoulos, * S., Tang, C. M., and Sprangle, P.				
13a. TYPE OF REPORT Interim	13b. TIME COVERED FROM TO	14. DATE OF REPORT (Year, Month, Day) 1987 May 20	15. PAGE COUNT 28	
16. SUPPLEMENTARY NOTATION *Science Applications Intl. Corp., McLean, VA				
17. COSATI CODES			18. SUBJECT TERMS (Continue on reverse if necessary and identify by block number)	
FIELD	GROUP	SUB-GROUP	Maser, Short wavelength generators, Gyrotrons, Coherent radiation sources.	
19. ABSTRACT (Continue on reverse if necessary and identify by block number) <p>The induced resonance electron cyclotron (IREC) maser operates at Doppler upshifted frequencies $\omega = \gamma^2 \omega_0$, with γ the relativistic factor and $\omega_0 = eB/mc$. In addition, the mechanism is insensitive to the beam thermal spreads when the index of refraction $n = kc/\omega$ is properly adjusted. A set of simplified equations, describing the electron dynamics near the axis of the configuration, is derived in the limit of small Larmor radius. The linear efficiency is derived for radiation having a Gaussian profile and propagating at an angle α relative to a constant external magnetic field. The start-up current for operation in the submillimeter regime is well within the capabilities of today's long pulse relativistic electron beams.</p>				
20. DISTRIBUTION AVAILABILITY OF ABSTRACT <input checked="" type="checkbox"/> UNCLASSIFIED/UNLIMITED <input type="checkbox"/> SAME AS RPT <input type="checkbox"/> DTIC USERS			21. ABSTRACT SECURITY CLASSIFICATION UNCLASSIFIED	
22a. NAME OF RESPONSIBLE INDIVIDUAL C. M. Tang			22b. TELEPHONE (Include Area Code) (202) 767-4148	22c. OFFICE SYMBOL Code 4790

DD FORM 1473, 14 MAR

83 APR edition may be used until exhausted
All other editions are obsolete

SECURITY CLASSIFICATION OF THIS PAGE

GSA General Printing Office: 1005-207-607

CONTENTS

I.	INTRODUCTION	1
II.	FIELD AND PARTICLE DYNAMICS	2
III.	EFFICIENCY	5
	a. Small Signal Efficiency	6
	b. Start-up Current	9
IV.	CONCLUSION AND SUMMARY	10
	ACKNOWLEDGMENT	11
	REFERENCES	12



Accession For	
NTIS GRA&I	<input checked="" type="checkbox"/>
DTIC TAB	<input type="checkbox"/>
Unannounced	<input type="checkbox"/>
Justification	
By	
Distribution /	
Availability Codes	
Dist	Availability or Special
A-1	

SMALL SIGNAL ANALYSIS OF THE INDUCED RESONANCE ELECTRON CYCLOTRON MASER

I. Introduction

Generation of intense radiation in the microwave regime utilizing electron cyclotron interaction has been proposed independently by a number of researchers in the late 1950's.¹⁻⁴ Electrons gyrating in resonance with the radiation field can experience a bunching in the relative wave-particle phase through the dependence of the cyclotron frequency on the relativistic mass. High amplification of the radiation field, known as masing action, results for Doppler shifted frequencies slightly above the electron cyclotron frequency. Electron cyclotron masers, also called gyrotrons,⁵⁻³⁰ have demonstrated efficient high power generation of electromagnetic waves at centimeter wavelengths.

For many purposes it is of practical interest to develop high power generation capability at millimeter and submillimeter wavelengths. Potential areas of application include advanced accelerators, short wavelength radar, plasma heating in fusion reactors and spectroscopy. The shortest wavelength for single mode operation in a closed resonator is tied to the transverse dimension of the cavity. For radiation wavelengths much shorter than the transverse dimensions, a multimode excitation will result from the small frequency separation among nearby modes. The mode selectivity is greatly improved by the use of an open resonator configuration, the quasi-optical maser.^{19,20}

A new configuration has recently been proposed^{29,30} which utilizes the benefits of the open resonators and at the same time minimizes the detrimental effects of the injected electron beam energy spread. The operating frequency in the induced resonance electron

cyclotron (IREC) quasi-optical maser is upshifted by a factor γ^2 relative to the relativistic electron cyclotron frequency. It has been shown that for operation at the optimum index of refraction the efficiency is relatively insensitive to the beam energy spread and the sensitivity to the effect of pitch angle spread can be minimized. The index of refraction is adjustable by varying the angle between the resonators (see Fig. (1)) and the guide field, and can be chosen to minimize the effects of finite beam quality. Finally, by spatially tapering the magnetic field the operating efficiency can be increased.

In this paper we limit ourselves to analyzing the small signal efficiency characteristics of such a device. We include the effects of the Gaussian profile for the radiation envelope considering a uniform magnetic field for simplicity. Nonlinear effects and the role of the magnetic field tapering are treated elsewhere.³⁰

The remainder of this paper is organized as follows. In Sec. II we describe the field configuration and the equations of motion. In Sec. III we derive the linear energy, power efficiency and start-up current condition. In Sec. IV numerical results and conclusions are presented.

II. Field and Particle Dynamics

The configuration for the induced resonance electron cyclotron (IREC) quasi-optical maser is shown schematically in Fig. 1. The interaction cavity is formed by two quasi-optical resonators intersecting at an angle 2α where α is the angle relative to the external magnetic field B_0 in the z -direction.

The beam radius is much smaller than the Gaussian width r_0 (spot size) for the radiation envelope. In the limit of small Larmor radius ρ compared to the perpendicular wavelength $k_\perp \rho \ll 1$ we can approximate the vector potential in the interaction regime by

$$\begin{aligned} \underline{A}_T = & A_R(z) \exp[i\Phi(z,t)] \frac{1}{2} (\hat{e}_x + i\hat{e}_y) + cc \\ & + A_L(z) \exp[i\Phi(z,t)] \frac{1}{2} (\hat{e}_x - i\hat{e}_y) + cc. \end{aligned} \quad (1)$$

Since we are interested in the synchronous interaction of the gyrating electrons with the radiation, we have kept only the forward propagating wave component $\Phi(z,t) = k_z z - \omega t + \Phi_0$. The amplitudes A_R and A_L for the right- and left-handed polarized wave component, respectively are given by

$$\begin{aligned} A_{R,L}(z) &= A_{R,L}^0 \exp[-z^2/L^2], \\ A_{R,L}^0 &= A_0 (\cos\alpha \pm 1), \\ L &= r_0/\sin\alpha, \end{aligned} \quad (2)$$

where A_0 and r_0 are the amplitude and spot size for each individual resonator beam.

We use the guiding center description for the particle orbits

$$\begin{aligned} x &= x_g + \rho \sin\zeta, & y &= y_g - \rho \cos\zeta, \\ p_x &= p_{gx} + p_\perp \cos\zeta, & p_y &= p_{gy} + p_\perp \sin\zeta, \end{aligned} \quad (3)$$

to obtain the nonlinear relativistic equations of motion. In this representation (x_g, y_g) and (p_{gx}, p_{gy}) denote the transverse coordinates

and momentum of the particle's guiding center, ρ is the Larmor radius, p_{\perp} is the magnitude of the transverse momentum and ζ is the momentum space angle. We assume that x , y , p_x , p_y , ρ and p_{\perp} are slowly changing, on the spatial scale of a gyroperiod. An additional condition for ignoring finite k_{\perp} effects is that the guiding center shift in the x direction be small $k_{\perp}\Delta x \ll 1$, valid for $\alpha \ll 1$ where k_{\perp} is $k \sin \alpha$. Using the Lorentz force equation together with Maxwell's equations and retaining only the right-hand polarized wave component the nonlinear relativistic equations of motion are cast into the form

$$u_1' = - [(\omega\gamma/cu_z) - k_z] a(z) \cos\psi + a'(z) \sin\psi, \quad (4a)$$

$$u_z' = - (u_1/u_z) [k_z a(z) \cos\psi + a'(z) \sin\psi], \quad (4b)$$

$$\psi' = - (\gamma\Delta\omega/cu_z) + (1/u_1) \left[\left[(\omega\gamma/cu_z) - k_z \right] a(z) \sin\psi + a'(z) \cos\psi \right], \quad (4c)$$

The prime (') in Eqs. (4) signifies the d/dz derivative, $u = p/m_0c = \gamma\beta/c$, $\gamma = (1 + u_1^2 + u_z^2)^{1/2}$ is the relativistic mass factor, $a(z) = |e|A_R(z)/m_0c^2$ is the normalized radiation amplitude, $\psi = \zeta + \phi$ is the relative phase between the radiation field and particle, $n = ck_z/\omega = \cos\alpha$ is the refractive index associated with the radiation field, $\Delta\omega = [\omega(1-n\beta_z) - \Omega_0/\gamma]$ is the frequency mismatch term and $\Omega_0 = |e|B_0/m_0c$ is the nonrelativistic electron cyclotron frequency. Using Eqs. (4) the rate of change of γ is given by

$$\gamma' = - \omega(u_1/cu_z) a(z) \cos\psi. \quad (5)$$

The frequency mismatch $\Delta\omega$ and its dependence on the particle energy through the relativistic correction γ , provide the mechanism for the masing action (phase bunching).

III. Efficiency

One of the central issues concerning maser operation is the efficiency of the configuration. Efficiency calculations have been carried out for various configurations in the general categories of the closed resonator gyrotron^{5-18,21-28} or the open resonator quasi-optical maser.^{19,20} While it is generally recognized that nonlinear saturation mechanisms are very important for the full power operation, it is useful to carry out the small signal efficiency calculation in order to compute the start-up current. Expressions for the small amplitude efficiency, obtained in closed form, provide some guidelines in selecting the optimum operating parameters.

Assuming steady state operation, with the number of particles crossing the unit area per unit time $n_0 v_z$ being constant, the efficiency can be defined by

$$\eta_E = - \left\langle \frac{\gamma_f - \gamma_0}{\gamma_0 - 1} \right\rangle = \langle \gamma_0 - 1 \rangle^{-1} \int d^3 p_0 f_0(p_0) \int_{-\infty}^{\infty} dz \frac{\partial \gamma}{\partial z}. \quad (6)$$

In Eq. (6), the bracket $\langle \rangle$ signifies the average over the initial distribution in phase space, the subscript $\pm\infty$ stands for the initial and final values at $z = \pm\infty$ respectively and $\partial\gamma/\partial z$ is a function of the initial conditions $\gamma = \gamma(z; p_{\perp 0}, p_{z0}, \psi_0)$. In the cold beam limit with the initial distribution function given by $f_0(p_{\perp}, p_z, \psi) = (n_0/2\pi p_{\perp}) \delta(p_{\perp} - p_{\perp 0}) \delta(p_z - p_{z0})$ the average reduces to an average over $\psi_0 = \zeta_0 + \phi_0$.

a. Small Signal Efficiency

We proceed to compute the small signal power efficiency by evaluating the right-hand side of Eq. (6) using Eq. (5). A first order expansion for the quantities $u_{\perp} = u_{\perp}^{(0)} + u_{\perp}^{(1)}$, $\gamma = \gamma^{(0)} + \gamma^{(1)}$, $\psi = \psi^{(0)} + \psi^{(1)}$ will suffice for a quadratic expression in the wave amplitude a . The integrand on the right-hand side of Eq. (6) is expanded using the linear solutions from Eqs. (4a)-(4c). The evaluation of the final result is considerably simplified by performing the phase space average over the angle ψ_0 before the spatial integration over z . Expanding the products of the trigonometric terms inside the integral in Eq. (6) into sums and averaging over ψ_0 leads to

$$\begin{aligned} \left\langle \int_{-\infty}^{\infty} dz \frac{\partial \gamma}{\partial z} \right\rangle = & - \left(\frac{\omega}{cu_{z0}} \right) \left[\left(1 + \frac{1}{2} \frac{u_{\perp 0}^2}{u_{z0}^2} \right) \int_{-\infty}^{\infty} dz a(z) \int_{-\infty}^z dz' \frac{da(z')}{dz'} \sin \Delta_0(z-z') \right. \\ & + \left\{ k_z \left(1 + \frac{1}{2} \frac{u_{\perp 0}^2}{u_{z0}^2} \right) - \frac{\omega \gamma_0}{cu_{z0}} \right\} \int_{-\infty}^{\infty} dz a(z) \int_{-\infty}^{\infty} dz' a(z') \cos \Delta(z-z') \\ & - \frac{1}{2} \left\{ \frac{\omega^2}{c^2} \frac{u_{\perp 0}^2}{u_{z0}^2} - k_z \frac{u_{\perp 0}^2}{u_{z0}^2} \left(\frac{\omega \gamma_0}{cu_{z0}} - \frac{Q_0}{cu_{z0}} \right) \right\} \int_{-\infty}^{\infty} dz a(z) \int_{-\infty}^z dz' \int_{-\infty}^{z'} dz'' a(z'') \sin \Delta_0(z-z'') \\ & \left. + \frac{1}{2} \frac{u_{\perp 0}^2}{u_{z0}^2} \left(\frac{\omega \gamma_0}{cu_{z0}} - \frac{Q_0}{cu_{z0}} \right) \int_{-\infty}^{\infty} dz a(z) \int_{-\infty}^z dz' \int_{-\infty}^{z'} dz'' \frac{da(z'')}{dz''} \cos \Delta_0(z-z'') \right], \quad (7) \end{aligned}$$

$$\text{where } \Delta_0 = \frac{Q_0}{cu_{z0}} - \left(\frac{\omega \gamma_0}{cu_{z0}} - k_z \right) = - \frac{\Delta \omega_0}{v_{z0}}, \quad a(z) = a_0 \exp[-z^2/L^2]$$

$$\text{and } a_0 = |e| A_R^0 / m_0 c^2.$$

We evaluate the remaining integrals in Eq. (14) and express the final result in terms of the parameters $\xi = \omega\tau = (\omega\gamma_0/cu_{z0})L$, τ being the transit time through the interaction regime, and the relative frequency mismatch $\Delta\omega_0/\omega$. We find

$$\begin{aligned} \eta_p = & \frac{\pi}{2} \frac{a_0^2 \xi^2}{\gamma_0(\gamma_0-1)} \left\{ (1 + \theta_0^2) n \beta_{z0}^{-1} \right. \\ & + \left[\frac{1}{2} \xi^2 \beta_{10}^2 (1 - n^2) + (1 + \theta_0^2) \right] \frac{\Delta\omega_0}{\omega} - \theta_0^2 n \beta_{z0} \xi^2 \left(\frac{\Delta\omega_0}{\omega} \right)^2 \\ & \left. - \frac{\theta_0^2}{2} \xi^2 \left(\frac{\Delta\omega_0}{\omega} \right)^3 \right\} e^{-\frac{1}{2} \xi^2 \frac{\Delta\omega_0^2}{\omega^2}}, \end{aligned} \quad (8)$$

with $\theta_0 = u_{10}/u_{z0}$, the initial pitch angle.

The efficiency is proportional to $\exp[-1/2 \xi^2 \Delta\omega_0^2/\omega^2]$ where exponent $\xi(\Delta\omega_0/\omega)$ is equal to $\Delta\omega_0\tau$, the advance in the relative phase $\Delta\psi_0$ between the wave and the particle over the interaction regime. For typical values of $\xi \gg 1$ and $\Delta\omega_0/\omega \ll 1$ the expression in braces in Eq. (8) is simplified to

$$\left\{ \dots \right\} = (1 + \theta_0^2) n \beta_{z0}^{-1} + \frac{\xi_0^2 \beta_{10}^2}{2} \frac{\Delta\omega_0}{\omega} - \theta_0^2 \beta_{z0} \frac{\xi_0^2}{\sin^2 \alpha} \left(\frac{\Delta\omega_0}{\omega} \right)^2, \quad (9)$$

where $\xi_0^2 = \xi^2 (1 - n^2)$ is independent of α . In (9) we have omitted the small terms that originate from the gradient terms $\partial a/\partial z$ in the equations of motion. Treating (9) as a quadratic form in $\Delta\omega/\omega$ we find the regime for positive efficiency, given by

$$2 \left(1 - (1 + \theta_0^2) n \beta_{z0} \right) \left(\beta_{10}^2 \xi_0^2 \right)^{-1} < \frac{\Delta\omega_0}{\omega} < \beta_{10}^2 (1 - n^2) \left(n \theta_0^2 \beta_{z0} \right)^{-1}. \quad (10)$$

The upper limit in $\Delta\omega_0/\omega$ is due to a finite n and results from the negative contribution of the quadratic term $(\Delta\omega/\omega)^2$ that overtakes the positive contribution of the linear term $\Delta\omega/\omega$ for small angles $\sin^2\alpha < (2n\theta_0^2\beta_{z0}/\beta_{10}^2) (\Delta\omega_0/\omega)$.

In order to determine the maximum efficiency within the positive regime, we parameterize Eq.(8) as a function of $x = \xi \Delta\omega/\omega$, since the exponential is the main factor limiting efficiency. Setting $d\eta/dx = 0$, we obtain

$$c_3 x^3 - c_2 x^2 - c_1 x + c_0 = 0, \quad (11)$$

with $c_1 = (1 + 3\theta_0^2)\beta_{z0} \cos\alpha - 1$, $c_3 = \theta_0^2\beta_{z0} \cos\alpha$ and $c_2 = c_0 = (1/2) \beta_{10}^2 \xi_0 \sin\alpha$. Observing that the terms proportional to c_1 and c_3 can be omitted provided that $c_0 = c_2 \gg c_3 \sim c_1 \sim 1$ or

$$\sin\alpha \gg \frac{\theta_0^2 \beta_{z0}}{\beta_{10}^2 \xi_0}, \quad (12)$$

we can show that $x \approx 1$. In the special case $x = 1$, we obtain the maximum efficiency

$$\eta_{\max} = \frac{\pi}{4} a_0^2 e^{-1/2} \frac{\beta_{10}^2 \xi_0^3}{\gamma_0(\gamma_0 - 1)} (\sin\alpha)^{-1}. \quad (13)$$

The overall efficiency increases with decreasing α (increasing index of refraction) provided that inequality Eq. (12) remains valid. For very small α Eq. (13) fails and a solution of the cubic Eq. (11) is necessary.

b. Start-up Current

We are in position now to calculate the start-up beam current utilizing the power efficiency coefficient. Amplification of the electromagnetic field energy will result if

$$\eta P_b > \frac{d\varepsilon}{dt}, \quad (14)$$

where ε is the total electromagnetic energy stored in both cavities $\varepsilon = \int U_R dV = 2V(\omega^2/c^2)(A_0^2/4\pi)$, $V = \pi r_0^2 L_T$, $d\varepsilon/dt = (\omega/Q)\varepsilon$, Q is the quality factor for the cavity and P_b is the electron beam power.

The optimum power efficiency η_{\max} is given by Eq. (13). The cavity Q is given by

$$Q = \frac{2\pi}{1-R_{ef}} \frac{L_T}{\lambda}, \quad (15)$$

where L_T is the effective resonator length and λ the wavelength. Combining Eqs. (13), (14), (15) and expressing A_0 in terms of a_0 from Eq. (2) we obtain

$$P_b > \frac{\lambda}{r_0} (1-R_{ef}) \frac{\exp(\frac{1}{2})}{4\pi^2} \frac{m_0^2 c^5}{|e|^2} \frac{\beta_{z0}^3 \gamma_0 (\gamma_0 - 1)}{\beta_{l0}^2} \frac{2 \sin \alpha}{(1 + \cos \alpha)^2}, \quad (16)$$

where $P_b = I_b V_b$, I_b is the current and V_b is voltage of the electron beam. For typical parameters $V_b = 0.25 \times 10^6 \text{ eV}$, $\lambda/r_0 = 10^{-1}$, $1-R_{ef} = 0.1$, $\gamma_0 = 1.5$, $\beta_{z0} \approx 0.64$, $\beta_{l0} = (\sqrt{3}\gamma_0)^{-1}$, and the optimum operation angle $\alpha \approx 45^\circ$, the start-up current is

$$I_b \geq 4.6 \text{ A.}$$

IV. Conclusion and Summary

We have performed the small signal analysis for an oscillator configuration capable of generating radiation in the millimeter and the submillimeter regime. The threshold for the start-up current was found to be well within the existing capabilities of today's long pulse mildly relativistic beams. Our theoretical linear efficiency results are plotted as solid lines in Figs. 2-4 against the numerical results (dots) obtained by direct integration of the fully nonlinear Eqs. (4) for small wave amplitude. Plots of the linear efficiency as a function of the controlling parameter $\xi \Delta\omega/\omega$ for constant radiation amplitude a_0 and constant spot size r_0 are shown in Fig. 2, with each curve corresponding to a different index of refraction $n = \cos\alpha$. The maximum efficiency for all plots occurs at $\xi \Delta\omega/\omega \approx 1$ in agreement with Eq. (13). Small signal efficiency increases with increasing $n = \cos\alpha$ roughly proportionally to the length of the interaction regime $L = r_0/\sin\alpha$. In Fig. 3, the optimum index of refraction ²⁹⁻³⁰ $n = \beta_{z0}/(1-\beta_{10}^2)$, to minimize the effects of beam energy spread, is held constant, and the interaction length L is changed by increasing the width of the radiation envelope r_0 . Figure 4 is a comparison of the theoretical small signal efficiency with the numerically calculated nonlinear efficiency as a function of wave amplitude a_0 . The agreement is good for $a_0 \leq 3 \times 10^{-4}$. Nonlinear saturation occurs for $a_0 > 1 \times 10^{-3}$. Obtaining the scaling of the efficiency in the nonlinear regime is not possible analytically. Numerical studies of the high power performance, however, have demonstrated good nonlinear efficiency.

Acknowledgment

This work is sponsored by the Department of Energy under Contract
Number DE-AI05-83ER40117.

References

1. R. Q. Twiss, Aust. J. Phys. 11, 564 (1958).
2. A. V. Gaponov, Isv. Vyssh. Uchebn. Zaved, Radiofiz., 2, 450 (1959).
3. R. H. Pantell, Proc. IRE, 47, 1146 (1959).
4. J. Schneider, Phys. Rev. Lett. 2, 504 (1959).
5. J. L. Hirshfield and J. M. Wachtel, Phys. Rev. Lett. 12, 533 (1964).
6. A. V. Gaponov, M. I. Petelin and V. K. Yulpatov, Radiophys. Quantum Electron. 10, 794 (1967).
7. V. L. Bratman, M. A. Moiseev, M. I. Petelin and R. E. Erm, Radiophys. Quantum Electron. 16, 474 (1973).
8. D. V. Kisel', G. S. Korablev, V. G. Navel'yev, M. I. Petelin and Sh. Ye. Tsimring, Radio Eng. Electron. Phys. 19, No. 4, 95 (1974).
9. N. I. Zaytsev, T. B. Pankratova, M. I. Petelin and V. A. Flyagin, Radio Eng. Electron. Phys. 19, No. 5, 103 (1974).
10. V. L. Granatstein, M. Herndon, R. K. Parker and P. Sprangle, IEEE J. Quantum Electron. QE-10 p. 651 (1974).
11. E. Ott and W. M. Manheimer, IEEE Trans. Plasma Science PS-3, 1 (1975).
12. V. L. Granatstein, P. Sprangle, R. K. Parker, and M. Herndon, J. Appl. Phys. 46, 2021 (1975).
13. P. Sprangle and W. M. Manheimer, Phys. Fluids 18, 224 (1975).
14. P. Sprangle and A. T. Drobot, IEEE Trans. Microwave Theory and Techniques MTT-25, 528 (1977).
15. J. L. Hirshfield and V. L. Granatstein, IEEE Trans. Microwave Theory and Tech. MTT-25, 522 (1977).
16. K. R. Chu and J. L. Hirshfield, Phys. Fluids 21, 461 (1978).

17. V. L. Bratman, N. S. Ginzburg and M. I. Petelin. Optics Commun. 30, 409 (1979).
18. P. Sprangle and R. A. Smith, J. Appl. Phys. 51, p. 3001 (1980).
19. P. Sprangle, J. L. Vomvoridis and W. M. Manheimer, Appl. Phys. Lett. 38, 5, p. 310 (1981), also Phys. Rev. A23, 3127 (1981).
20. J. L. Vomvoridis and P. Sprangle, Phys. Rev. A25, 931 (1982).
21. K. E. Kreischer and R. J. Temkin, Intl. J. of Infrared and Millimeter Waves, 2, p. 175 (1981).
22. V. L. Bratman, N. S. Ginzburg, G. S. Nusinovich, M. I. Petelin and P. S. Strelkov, Intl. J. Electron. 51, 541 (1981).
23. I. E. Botvinnik, V. L. Bratman, A. B. Volkov, N. S. Ginzburg, G. G. Denisov, B. D. Kol'chugin, M. N. Ofitserov and M. I. Petelin, JETP Lett. 35, p. 516 (1982).
24. Y. Y. Lau, IEEE Trans., ED-29, p. 320 (1982).
25. V. L. Bratman, G. G. Denisov, N. S. Ginzburg and M. I. Petelin, IEEE J. Quantum Electron, QE-19, 282 (1983).
26. A. T. Lin, W. W. Chang and C.-C. Lin, Phys. Fluids 27, 1054 (1984).
27. C. S. Wu and L. C. Lee, Astrophysical Journal 230, 621 (1979).
28. B. Levush, A. Bondeson, W. M. Manheimer and E. Ott, Intl. J. Electr. 54, 749 (1983).
29. P. Sprangle, C. M. Tang and P. Serafini, NRL Memo Report No. 5678 (1986), also in Nucl. Instr. and Methods in Phys. Res., A250, 361 (1986).
30. P. Sprangle, C.-M. Tang and P. Serafini, Appl. Phys. Lett. 49 (18) 1154 (1986).

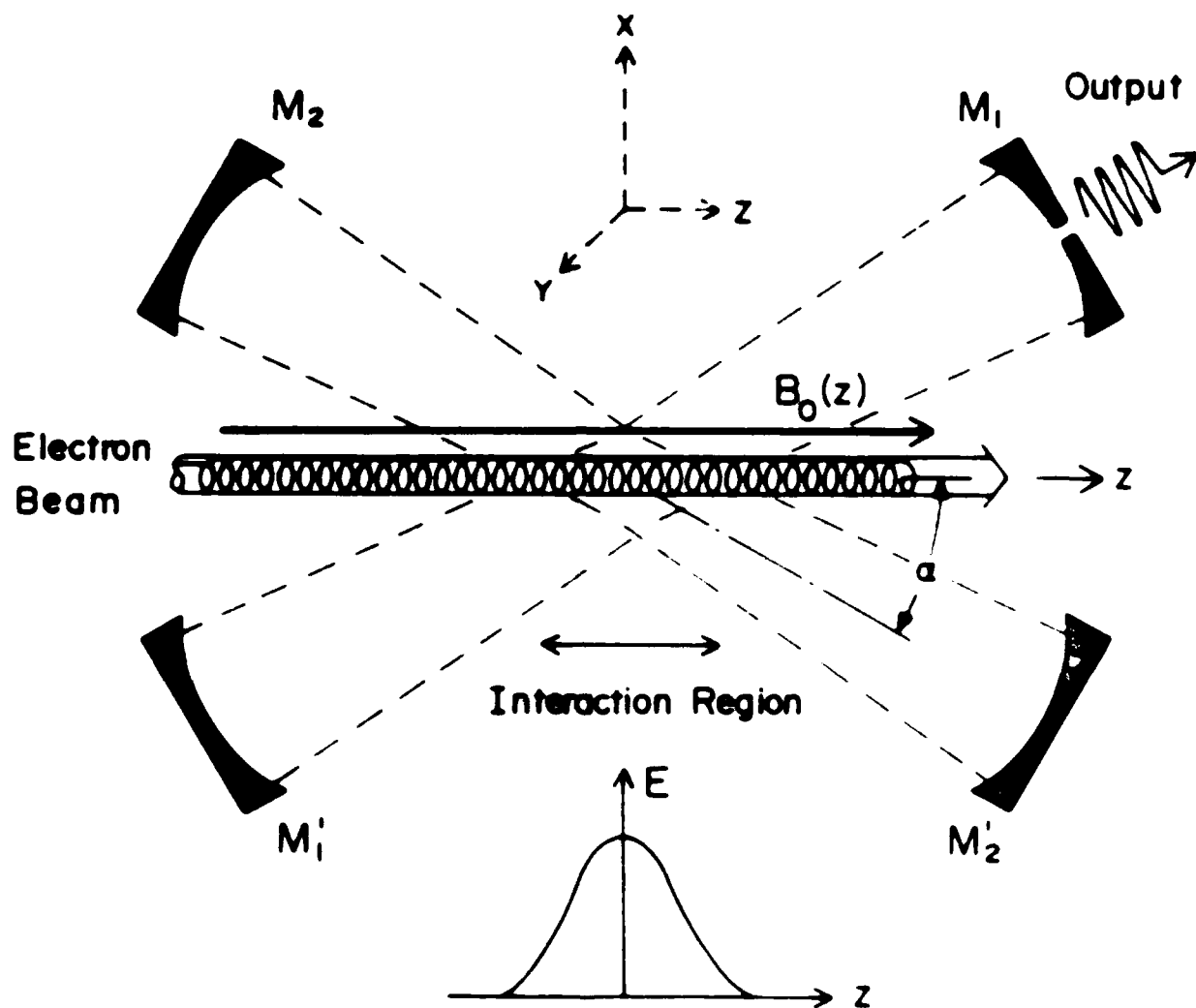


Figure 1. The configuration of the Induced Electron Resonance Maser.

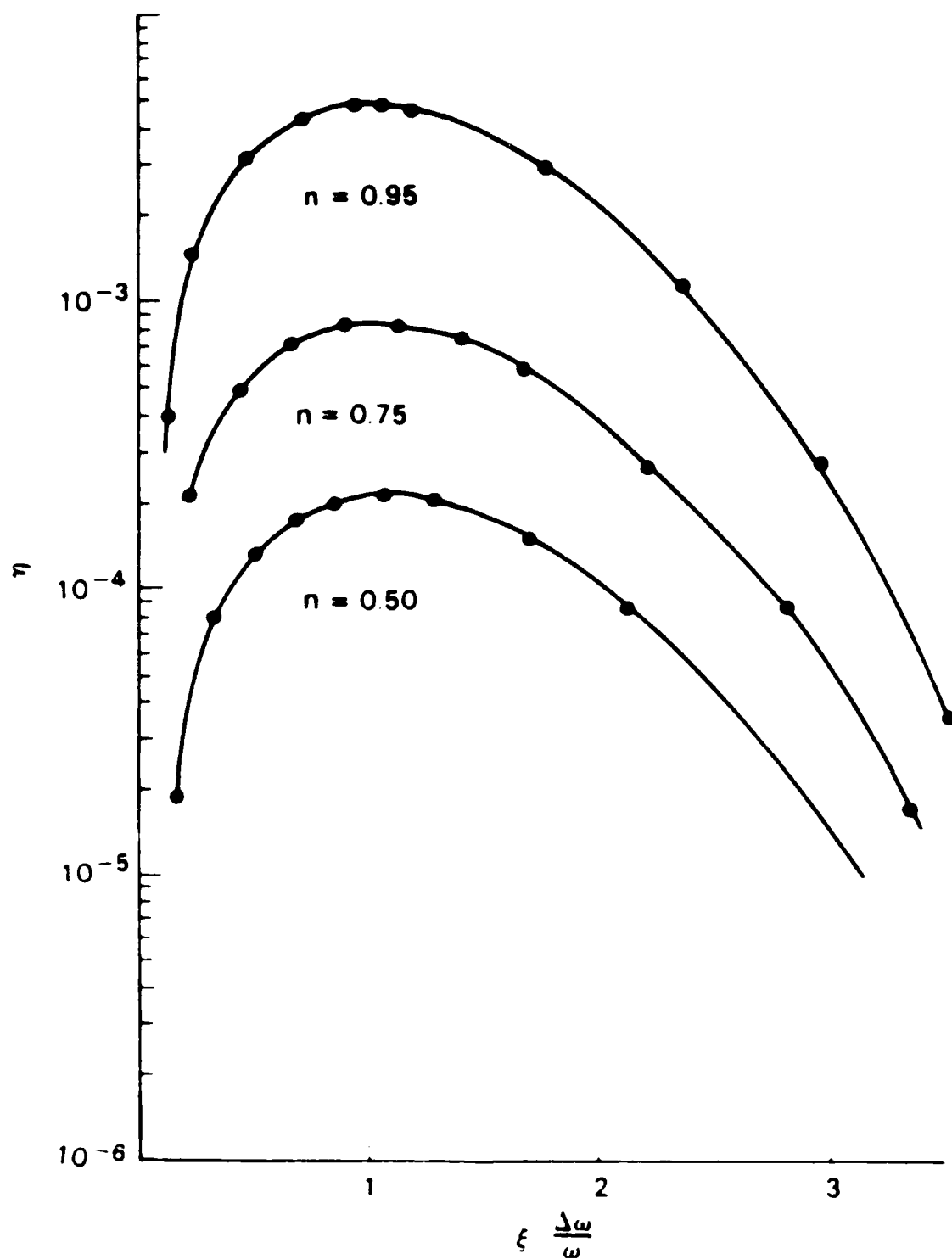


Figure 2. Theoretical (solid line) and numerical (dots) plots of linear efficiency η versus $\xi \frac{\Delta\omega}{\omega}$ for various values of index of refraction n with constant amplitude $a_0 = 5 \times 10^{-5}$ and $\nu = 1.5$.

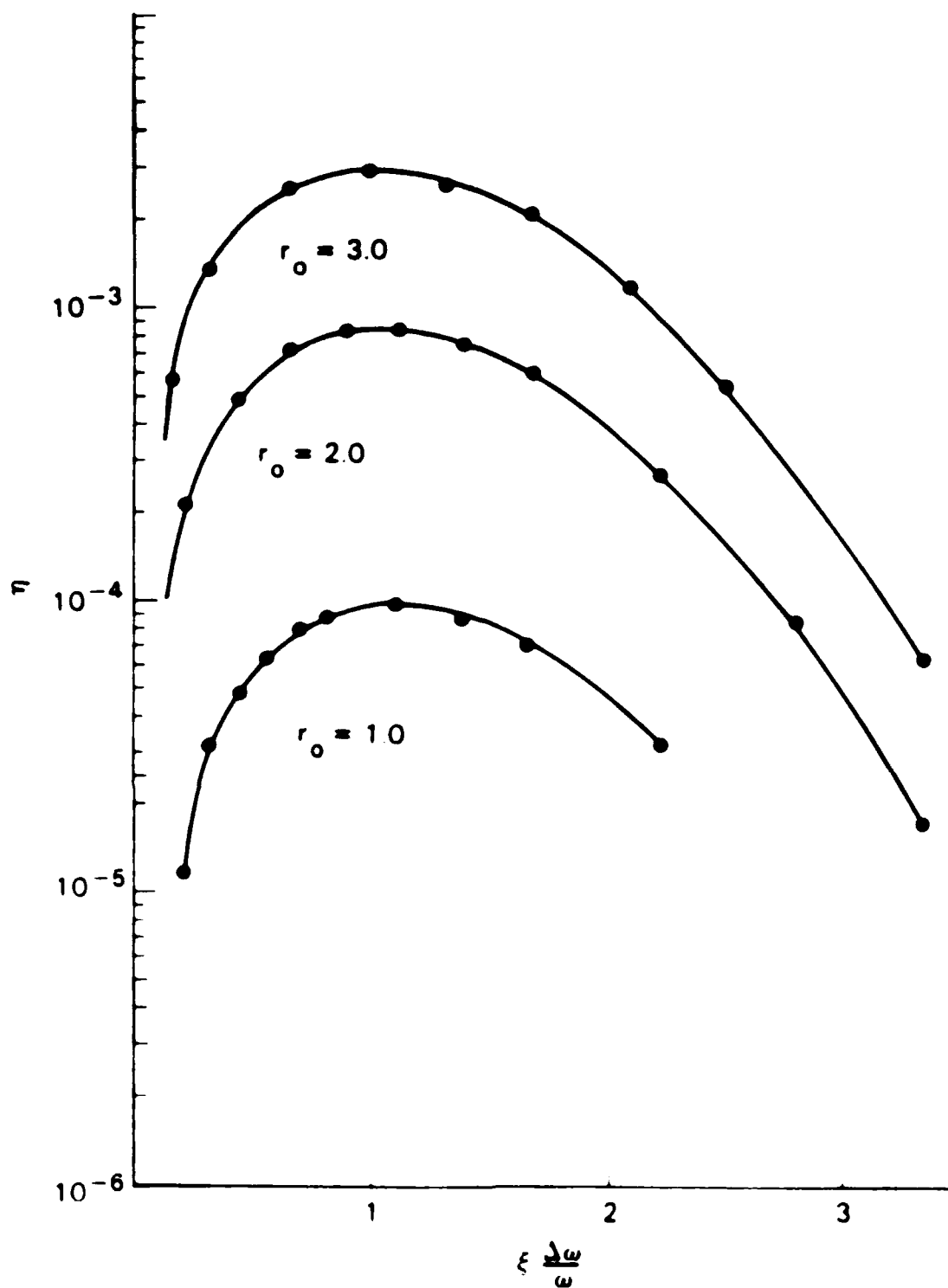


Figure 3. Theoretical (solid line) and numerical (dots) plots of linear efficiency η versus $\xi \frac{\Delta\omega}{\omega}$ for various Gaussian widths r_0 with constant refraction index n_{opt} and $a_0 = 5 \times 10^{-5}$, $\nu = 1.5$.

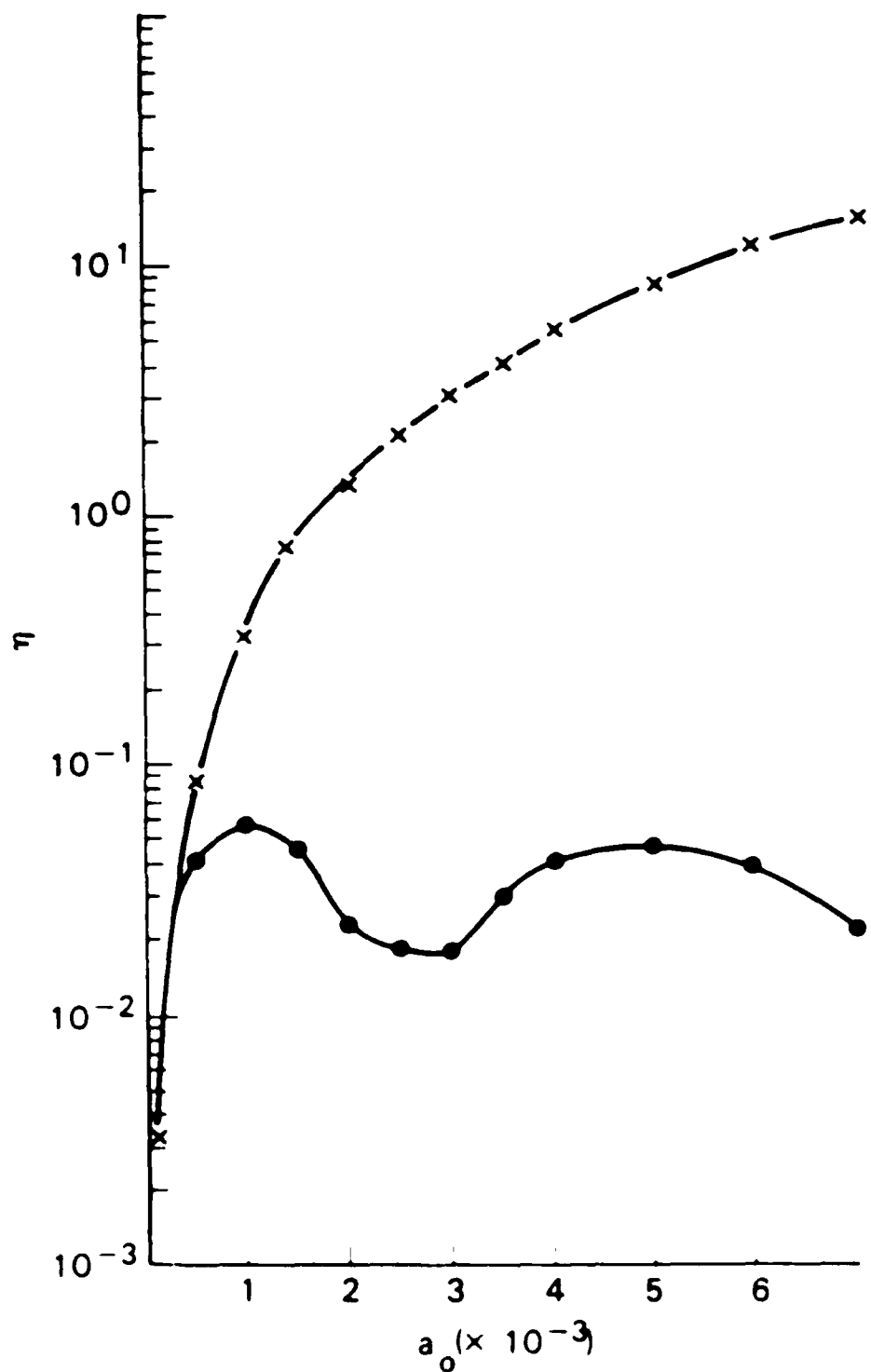


Figure 4. Comparison of linear (crosses) versus nonlinear (dots) efficiency η as a function of a_0 for $\xi = \Delta\omega/\omega = 1$, $\gamma = 0.75$ and $\nu = 1.5$.

DISTRIBUTION LIST

Naval Research Laboratory
4555 Overlook Avenue, S.W.
Washington, DC 20375-5000

Attn: Code 1000 - CAPT William C. Miller
1001 - Dr. T. Coffey
4603 - Dr. W.W. Zachary
4700 - Dr. S. Ossakow (26 copies)
4710 - Dr. J.A. Pasour
4710 - Dr. C.A. Kapetanakos
4740 - Dr. W.M. Manheimer
4740 - Dr. S. Gold
4790 - Dr. P. Sprangle (100 copies)
4790 - Dr. C.M. Tang (50 copies)
4790 - Dr. M. Lampe
4790 - Dr. Y.Y. Lau
4790A- W. Brizzi
4730 - Dr. R. Elton
6652 - Dr. N. Seeman
6840 - Dr. S.Y. Ahn
6840 - Dr. A. Ganguly
6840 - Dr. R.K. Parker (5 copies)
6850 - Dr. L.R. Whicker
6875 - Dr. R. Wagner
2628 - Documents (20 copies)
2634 - D. Wilbanks
1220 - 1 copy

Dr. R. E. Aamodt
Science Applications Intl. Corp.
1515 Walnut Street
Boulder, CO 80302

Dr. B. Amini
1763 B. H.
U. C. L. A.
Los Angeles, CA 90024

Dr. D. Bach
Los Alamos National Laboratory
P. O. Box 1663
Los Alamos, NM 87545

Dr. L. R. Barnett
3053 Merrill Eng. Bldg.
University of Utah
Salt Lake City, UT 84112

Dr. Peter Baum
General Research Corp.
P. O. Box 6770
Santa Barbara, CA 93160

Dr. Russ Berger
FL-10
University of Washington
Seattle, WA 98185

Dr. B. Bezzerides
MS-E531
Los Alamos National Laboratory
P. O. Box 1663
Los Alamos, NM 87545

Dr. Mario Bosco
University of California, Santa Barbara
Santa Barbara, CA 93106

Dr. Howard E. Brandt
Department of the Army
Harry Diamond Laboratory
2800 Powder Mill Road
Adelphi, MD 20783

Dr. Bob Brooks
FL-10
University of Washington
Seattle, WA 98195

Dr. Paul J. Channell
AT-6, MS-H818
Los Alamos National Laboratory
P. O. Box 1663
Los Alamos, NM 87545

Dr. A. W. Chao
Stanford Linear Accelerator Center
Stanford University
Stanford, CA 94305

Dr. Francis F. Chen
UCLA, 7731 Boelter Hall
Electrical Engineering Dept.
Los Angeles, CA 90024

Dr. K. Wendell Chen
Center for Accel. Tech.
University of Texas
P.O. Box 19363
Arlington, TX 76019

Dr. Pisin Chen
S.L.A.C.
Stanford University
P.O. Box 4349
Stanford, CA 94305

Major Bart Clare
USASDC
P. O. Box 15280
Arlington, VA 22215-0500

Dr. Christopher Clayton
UCLA, 7731 Boelter Hall
Electrical Engineering Dept.
Los Angeles, CA 90024

Dr. Bruce I. Cohen
Lawrence Livermore National Laboratory
P. O. Box 808
Livermore, CA 94550

Dr. B. Cohn
L-630
Lawrence Livermore National Laboratory
P. O. Box 808
Livermore, CA 94550

Dr. Richard Cooper
Los Alamos National Laboratory
P. O. Box 1663
Los Alamos, NM 87545

Dr. Paul L. Csonka
Institute of Theoretical Sciences
and Department of Physics
University of Oregon
Eugene, Oregon 97403

Dr. J. M. Dawson
Department of Physics
University of California, Los Angeles
Los Angeles, CA 90024

Dr. A. Dimos
NW16-225
M. I. T.
Cambridge, MA 02139

Dr. J. E. Drummond
Western Research Corporation
8616 Commerce Ave
San Diego, CA 92121

Dr. Frank Felber
Jaycor
2055 Whiting Street
Alexandria, VA 22304

Dr. H. Figueroa
308 Westwood Plaza, No. 407
U. C. L. A.
Los Angeles, CA 90024

Dr. Jorge Fontana
Electrical and Computer Engineering Dept.
University of California at Santa Barbara
Santa Barbara, CA 93106

Dr. David Forslund
Los Alamos National Laboratory
P. O. Box 1663
Los Alamos, NM 87545

Dr. John S. Fraser
Los Alamos National Laboratory
P.O. Box 1663, MS H825
Los Alamos, NM 87545

Dr. Dennis Gill
Los Alamos National Laboratory
P. O. Box 1663
Los Alamos, NM 87545

Dr. B. B. Godfrey
Mission Research Corporation
1720 Randolph Road, SE
Albuquerque, NM 87106

Dr. P. Goldston
Los Alamos National Laboratory
P. O. Box 1663
Los Alamos, NM 87545

Prof. Louis Hand
Cornell University
Ithaca, NY 14853

Dr. J. Hays
TRW
One Space Park
Redondo Beach, CA 90278

Dr. Wendell Horton
University of Texas
Physics Dept., RLM 11.320
Austin, TX 78712

Dr. J. Y. Hsu
General Atomic
San Diego, CA 92138

Dr. H. Huey
Varian Associates
B-118
611 Hansen Way
Palo Alto, CA 95014

Dr. Robert A. Jameson
Los Alamos National Laboratory
AT-Division, MS H811
P.O. Box 1663
Los Alamos, NM 87545

Dr. G. L. Johnston
NW16-232
M. I. T.
Cambridge, MA 02139

Dr. Shayne Johnston
Physics Department
Jackson State University
Jackson, MS 39217

Dr. C. Joshi
Electrical Engineering Department
University of California, Los Angeles
Los Angeles, CA 90024

Dr. E. L. Kane
Science Applications Intl. Corp.
McLean, VA 22102

Dr. Tom Katsouleas
UCLA, 1-130 Knudsen Hall
Department of Physics
Los Angeles, CA 90024

Dr. Kwang-Je Kim
Lawrence Berkeley Laboratory
University of California, Berkeley
Berkeley, CA 94720

Dr. S. H. Kim
Center for Accelerator Technology
University of Texas
P.O. Box 19363
Arlington, TX 76019

Dr. Joe Kindel
Los Alamos National Laboratory
P. O. Box 1663, MS E531
Los Alamos, NM 87545

Dr. Ed Knapp
Los Alamos National Laboratory
P. O. Box 1663
Los Alamos, NM 87545

Dr. Norman M. Kroll
B-019
University of California, San Diego
La Jolla, CA 92093

Dr. Kenneth Lee
Los Alamos National Laboratory
P.O. Box 1663, MS E531
Los Alamos, NM 87545

Dr. N. C. Luhmann, Jr.
7702 Boelter Hall
U. C. L. A.
Los Angeles, CA 90024

Dr. K. Maffee
University of Maryland
E. R. B.
College Park, MD 20742

Dr. B. D. McDaniel
Cornell University
Ithaca, NY 14853

Dr. Warren Mori
1-130 Knudsen Hall
U. C. L. A.
Los Angeles, CA 90024

Dr. P. L. Morton
Stanford Linear Accelerator Center
P. O. Box 4349
Stanford, CA 94305

Dr. Robert J. Noble
S.L.A.C., Bin 26
Stanford University
P.O. Box 4349
Stanford, CA 94305

Dr. Craig L. Olson
Sandia National Laboratories
Plasma Theory Division 1241
P.O. Box 5800
Albuquerque, NM 87185

Dr. H. Oona
MS-E554
Los Alamos National Laboratory
P. O. Box 1663
Los Alamos, NM 87545

Dr. Robert B. Palmer
Brookhaven National Laboratory
Upton, NY 11973

Dr. Richard Pantell
Stanford University
308 McCullough Bldg.
Stanford, CA 94305

Dr. Claudio Pellegrini
National Synchrotron Light Source
Brookhaven National Laboratory
Upton, NY 11973

Dr. Melvin A. Piestrup
Adelphi Technology
13800 Skyline Blvd. No. 2
Woodside, CA 94062

Dr. Z. Pietrzyk
FL-10
University of Washington
Seattle, WA 98185

Dr. Don Prosnitz
Lawrence Livermore National Laboratory
P. O. Box 808
Livermore, CA 94550

Dr. R. Ratowsky
Physics Department
University of California at Berkeley
Berkeley, CA 94720

Dr. Stephen Rockwood
Los Alamos National Laboratory
P. O. Box 1663
Los Alamos, NM 87545

Dr. R. D. Ruth
Lawrence Berkeley Laboratory
University of California, Berkeley
Berkeley, CA 94720

Dr. Al Saxman
Los Alamos National Laboratory
P.O. Box 1663, MS E523
Los Alamos, NM 87545

Dr. George Schmidt
Stevens Institute of Technology
Department of Physics
Hoboken, NJ 07030

Dr. N. C. Schoen
TRW
One Space Park
Redondo Beach, CA 90278

Dr. Frank Selph
U. S. Department of Energy
Division of High Energy Physics, ER-224
Washington, DC 20545

Dr. Andrew M. Sessler
Lawrence Berkeley Laboratory
University of California, Berkeley
Berkeley, CA 94720

Dr. Richard L. Sheffield
Los Alamos National Laboratory
P.O. Box 1663, MS H825
Los Alamos, NM 87545

Dr. John Siambis
Lockheed Missiles & Space Co.
Bldg. 205, Dept. 92-20
3251 Hanover Street
Palo Alto, CA 94304

Dr. Sidney Singer
MS-E530
Los Alamos National Laboratory
P. O. Box 1663
Los Alamos, NM 87545

Dr. R. Siusher
AT&T Bell Laboratories
Murray Hill, NJ 07974

Dr. Jack Slater
Spectra Technology
2755 Northup Way
Bellevue, WA 98009

Dr. Todd Smith
Hansen Laboratory
Stanford University
Stanford, CA 94305

Dr. Richard Spitzer
Stanford Linear Accelerator Center
P. O. Box 4347
Stanford, CA 94305

Prof. Ravi Sudan
Electrical Engineering Department
Cornell University
Ithaca, NY 14853

Dr. Don J. Sullivan
Mission Research Corporation
1720 Randolph Road, SE
Albuquerque, NM 87106

Dr. David F. Sutter
U. S. Department of Energy
Division of High Energy Physics, ER-224
Washington, DC 20545

Dr. T. Tajima
Department of Physics
and Institute for Fusion Studies
University of Texas
Austin, TX 78712

Dr. Lee Teng, Chairman
Fermilab
P.O. Box 500
Batavia, IL 60510

Dr. H. S. Uhm
Naval Surface Weapons Center
White Oak Laboratory
Silver Spring, MD 20903-5000

U. S. Naval Academy (2 copies)
Director of Research
Annapolis, MD 21402

Dr. John E. Walsh
Wilder Laboratory
Department of Physics (HB 6127)
Dartmouth College
Hanover, NH 03755

Dr. Tom Wangler
Los Alamos National Laboratory
P. O. Box 1663
Los Alamos, NM 87545

Dr. Perry B. Wilson
Stanford Linear Accelerator Center
Stanford University
P.O. Box 4349
Stanford, CA 94305

Dr. W. Woo
Applied Science Department
University of California at Davis
Davis, CA 95616

Dr. Wendell Worton
Institute for Fusion Studies
University of Texas
Austin, TX 78712

Dr. Jonathan Wurtele
M.I.T.
NW 16-234
Plasma Fusion Center
Cambridge, MA 02139

Dr. M. Yates
Los Alamos National Laboratory
P. O. Box 1663
Los Alamos, NM 87545

Dr. Ken Yoshioka
Laboratory for Plasma and Fusion
University of Maryland
College Park, MD 20742

Dr. R. W. Ziolkowski, L-156
Lawrence Livermore National Laboratory
P. O. Box 808
Livermore, CA 94550

Contractors and Foreign

Dr. R. Bingham
Rutherford Appleton Laboratory
Chilton, Didcot
OX11 0QX
ENGLAND

Dr. Francesco De Martini
Istituto de Fisica
G. Marconi University
Piazzo delle Science, 5
ROMA 00185
ITALY

Dr. Roger G. Evans
Rutherford Appleton Laboratory
Chilton, Didcot
Oxfordshire OX11 0OX
GREAT BRITAIN

Dr. H. Hora
Department of Theoretical Physics
The University of New South Wales
Kensington-Sydney
Australia

Dr. D. A. Jones
Department of Theoretical Physics
The University of New South Wales
Kensington-Sydney
Australia

Dr. John D. Lawson
Rutherford High Energy Laboratory
Chilton
Didcot, Oxon OX11 0OX
ENGLAND

Dr. B. Luther-Davies
Australian National University
Canberra
AUSTRALIA

Dr. M. Masuzaki
Department of Physics
Kanazawa University
Kanazawa 920
JAPAN

Dr. A. Mondelli
Science Applications Intl. Corp.
1710 Goodridge Drive
McLean, VA 22101

Dr. Hans Motz
(Oxford University)
16, Bedford Street
Oxford OX4 1SU
GREAT BRITAIN

Dr. Alberto Renieri
Comitato Nazionale Energia Nucleare
Centro di Frascati
C.P. 65 - 00044
Frascati, Rome
ITALY

Dr. Robert Rossmanith
DESY
Hamburg 52
Notkestr 85
GERMANY

Dr. S. Solimeno
INFN Sez. di Napoli
Inst. di Fisica Sperimentale
Mostra d'Oltremare, Pad. 20
80125 Napoli,
ITALY

Dr. Thomas Weiland
DESY
Hamburg 52
Notkestr. 85
GERMANY

END

7-87

DTIC